(R1981) Evaluating the MHD Non-Newtonian Fluid Motion Past a Stretching Sheet Under the Influence of Non-uniform Thickness with Dufour and Soret Effects Implementing Chebyshev Spectral Method

M. M. Khader
Imam Mohammad Ibn Saud Islamic University (IMSIU)

Ram Prakash Sharma
NIT Arunachal Pradesh

Evaluating the MHD Non-Newtonian Fluid Motion Past A Stretching Sheet under the Influence of Non-uniform Thickness With Dufour and Soret Effects by Implementing Chebyshev Spectral Method

[1]**M. M. Khader and** [2]**Ram Prakash Sharma**

[1]Department of Mathematics and Statistics
College of Science
Imam Mohammad Ibn Saud Islamic
University (IMSIU)
Riyadh, Saudi Arabia
mmkhader@imamu.edu.sa

[2]Department of Mechanical Engineering
NIT Arunachal Pradesh, Yupia
Papum Pare District
Arunachal Pradesh-791112, India
ramprakash0808@gmail.com

Abstract

A study is made on the development of hydromagnetic non-Newtonian Casson and Williamson boundary layer flow in an electrically conducting fluid in the presence of heat flux, mass flux, and the uniform magnetic field. The governing non-linear system of PDEs is transformed into a set of non-linear coupled ODEs and then treated numerically by using the Chebyshev spectral method. The velocity, temperature, and concentration fields of the steady boundary layer flow, which are generated by the stretched sheet with non-uniform thickness are discussed. The simultaneous effects of the external magnetic field, Soret and Dufour phenomena with reference have been explored. The characteristic features of the flow phenomena are examined in some detail. Also, the main emphasis in the text of this paper was given to the structure of the friction factor, heat and mass transfer rates. The effect of different parameters, namely, magnetic number, Soret, Dufour parameters, Casson parameter, and Williamson parameter on velocity, thermal, and concentration distributions are discussed with the help of graphs. Finally, it is observed that the velocity decreases with an increase in the magnetic parameter. In addition, for the temperature profiles, opposite behavior is observed for increment in both the magnetic parameter and the Dufour parameter.

1. Introduction

In recent years, the study of hydrodynamic and hydromagnetic Casson or Williamson fluid flows has received considerable attention mainly due to the abundant geophysical and astrophysical applications (Zehra et al. (2015), Megahed (2015a)). Recent work on the analysis of Casson fluid mechanics has to lead to the introduction of the Casson number concept (Khan et al. (2017), Mahmoud and Megahed (2017), Megahed (2015b)). Megahed has introduced what is perhaps a more general concept, namely that of Williamson fluid flows with a perpetual rheological history (Megahed (2019), Megahed (2020)). Nadeem and Hussain (2014) discussed in some detail the concept of Williamson nanofluid history flows.

Recently, the heat and mass transfer (or double-diffusive) finds applications in a variety of engineering processes like in petroleum reservoirs, nuclear waste disposal, etc. The temperature gradient creates mass fluxes which is called thermo-diffusion or Soret effect, which is always found in the concentration equation. Additionally, the energy flux caused by a composition gradient is called the diffusion-thermo or Dufour effect, which can also exist in the energy equation. Generally, Dufour and Soret effects are of a smaller order of magnitude than the effects prescribed by Fourier law. As to the Soret and Dufour phenomena, special attention has been given to discussing them by various researchers (Mahmoud and Megahed (2013), Hayat et al. (2015) and Bidemi and Sami (2019)). By considering the variable thickness sheet, Lee (1967) was the first researcher who innovated the idea of the stretching sheet with variable thickness through tenuous needles. Later, studies on the variable thickness sheet were continued analytically by Fang et al. (2009) through the problems of MHD fluid flow past a shrinking/stretching sheet. Recently, many authors (Anjali and Prakash (2015), Anjali and Prakash (2016), and Khader and Megahed (2013)) deliberated various fluid flow problems across a stretching sheet with variable thickness.

So far no endeavor has been attempted towards the non-Newtonian Casson/Williamson MHD flow toward the slendering stretching sheet with heat mass flux within the sight of Soret and Dufour effects. So, to achieve this study, we use the well-known numerical technique, the Chebyshev-spectral method. Chebyshev polynomials are examples of eigenfunctions of singular Sturm-Liouville problems. Chebyshev polynomials have been used widely in the numerical solutions of the boundary value problems (Bell (1967)) and in computational fluid dynamics and many applications (Khader and Saad (2018a, 2018b), Khader and Abualnaja (2019), Khader (2013a, 2013b)). The existence of a fast Fourier transform for Chebyshev polynomials to efficiently compute matrix-vector products has meant that they have been more widely used than other sets of orthogonal polynomials. They are widely used because of their good properties in the approximation of functions.

The well-known family of orthogonal polynomials on $[-1, 1]$ are Chebyshev polynomials and can be determined with the aid of the following recurrence formula:

$$T_{n+1}(x) = 2x\, T_n(x) - T_{n-1}(x), \quad n = 1, 2, \dots.$$

The first three Chebyshev polynomials are $T_0(x) = 1$, $T_1(x) = x$, $T_2(x) = 2x^2 - 1$.

Khader and Sharma: Evaluating the MHD Non-Newtonian Fluid Motion

AAM: Intern. J., Vol. 17, Issue 2 (December 2022)   423

These polynomials have been implemented to solve the linear and non-linear differential equations and integro-differential equations (El-Gendi (1969)). This method is also adopted for solving the fractional diffusion equation (Khader (2011)) and fractional order integro-differential equations (Sweilam and Khader (2010)).

The organization of this paper is as follows. In the next section, the formulation of the problem is introduced. Section 3 summarizes the procedure solution using the Chebyshev spectral method. In Section 4 the results and discussion are given. Also, a conclusion is given in Section 5.

2.   Formulation of the Problem

Suppose the 2D laminar MHD flow of Casson and Williamson fluids flow over a stretched sheet with variable thickness. Here the x-axis is considered alongside the sheet motion and the y-axis is perpendicular to it. It is supposed that $y = A(x + b)^{\frac{1-m}{2}}$, $U_w(x) = U_0(x + b)^m$, $\nu_w = 0$, $m \neq 1$. This study does not take into account the induced magnetic field. The combined influence of Soret and Dufour impacts are considered. A transverse magnetic field of strength B_0 is employed. The physical model of the problem is depicted in Figure 1.
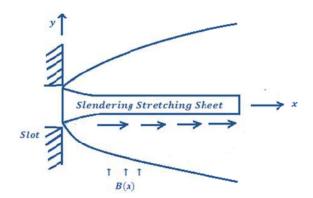

Figure 1. Physical description of the problem

With the above assumptions, the governing equations for steady 2D flow of Casson and Williamson fluids are expressed as:

$$\frac{\partial u}{\partial x} + \frac{\partial v}{\partial y} = 0, \tag{1}$$

$$u\frac{\partial u}{\partial x} + v\frac{\partial u}{\partial y} = v\left(1 + \frac{1}{\beta}\right)\frac{\partial^2 u}{\partial y^2} - \sqrt{2}\nu\Gamma\frac{\partial u}{\partial y}\frac{\partial^2 u}{\partial y^2} - \frac{\sigma\, B^2(x)}{\rho}u, \tag{2}$$

$$u\frac{\partial T}{\partial x} + v\frac{\partial T}{\partial y} = \frac{k}{\rho\, C_p}\frac{\partial^2 T}{\partial y^2} + \frac{D_m k_T}{C_s C_p}\frac{\partial^2 C}{\partial y^2}, \tag{3}$$

$$u\frac{\partial C}{\partial x} + v\frac{\partial C}{\partial y} = D_m \frac{\partial^2 C}{\partial y^2} + \frac{D_m k_T}{T_m}\frac{\partial^2 T}{\partial y^2}. \tag{4}$$

The corresponding boundary conditions are:

$$u = 0, \quad v = 0, \quad \frac{\partial T}{\partial y} = -\frac{h_w}{k}(T_w - T), \quad \frac{\partial C}{\partial y} = -\frac{h_s}{k}(C_w - C), \quad \text{at} \quad y = 0, \tag{5}$$

$$u \to U(x), \quad T \to T_\infty, \quad C \to C_\infty, \quad \text{as} \quad y \to \infty, \tag{6}$$

where h_w and h_s are transfers of the convective energy and the concentration coefficients, respectively; C_w and T_w are convective fluid concentration and temperature under the moving sheet, respectively.

We now suggest the following similarity transformations:

$$\psi(x, y) = f(\eta)\left(\frac{2}{m+1}\nu\, U_0 (x+b)^{m+1}\right)^{0.5}, \tag{7}$$

$$\eta = y\left(\frac{m+1}{2}U_0\frac{(x+b)^{m+1}}{\upsilon}\right)^{0.5}, \tag{8}$$

$$\theta(T_w(x) - T_\infty) = T - T_\infty, \qquad \phi(C_w(x) - C_\infty) = C - C_\infty. \tag{9}$$

If stream function ψ is described as $u = \frac{\partial\psi}{\partial y}$ and $v = -\frac{\partial\psi}{\partial x}$, then u and v satisfy the equation of continuity and become:

$$u = U_0(x+b)^m f'(\eta), \qquad v = -\sqrt{\frac{m+1}{2}\nu\, U_0(x+b)^{m-1}}\left[f'(\eta)\eta\left(\frac{m-1}{m+1}\right) + f(\eta)\right], \quad (10)$$

with the help of (7)-(10), Equations (2)-(4) converted as the below nonlinear system of ODEs:

$$\left(1+\frac{1}{\beta}\right)f''' + f''f - \left(\frac{2m}{m+1}\right)f'^2 + \Lambda\, f''f''' - M f' = 0, \tag{11}$$

$$\theta'' - Pr\left(\frac{1-m}{m+1}\right)f'\theta + Pr\, f\theta' + Pr\, Du\, \phi'' = 0, \tag{12}$$

Khader and Sharma: Evaluating the MHD Non-Newtonian Fluid Motion

AAM: Intern. J., Vol. 17, Issue 2 (December 2022)   425

$$\phi'' - Sc\left(\frac{1-m}{m+1}\right)f'\phi + Sc\,f\phi' + Sc\,Sr\,\theta'' = 0. \tag{13}$$

The non-dimensional form of boundary conditions can be written as:

$$f(0) = 0, \quad f'(0) = 0, \quad \theta'(0) = Bi1[1 - \theta(0)], \quad \phi'(0) = Bi2[1 - \phi(0)], \tag{14}$$

$$f'(\eta) \to 1, \quad \theta(\eta) \to 0, \quad \phi(\eta) \to 0, \quad \text{as } \eta \to \infty, \tag{15}$$

where Λ, M, Pr, Du, Sc, Sr, $Bi1$, $Bi2$ are defined as:

$$\Lambda = \Gamma\sqrt{(m+1)U_0^3\frac{(x+b)^{3m-1}}{\nu}}, \quad M = \frac{2\sigma\,B_0^2}{\rho\,U_0(m+!)}, \quad Pr = \frac{\mu\,C_p}{k},$$

$$Du = \frac{D_m k_T(C_w - C_\infty)}{\nu\,C_s C_p(T_w - T_\infty)}, \qquad Sc = \frac{\nu}{D_m}, \qquad Sr = \frac{D_m k_T(T_w - T_\infty)}{\nu\,T_m(C_w - C_\infty)}, \tag{16}$$

$$Bi1 = \frac{h_w}{k}\sqrt{\frac{\nu}{a}}, \qquad\qquad Bi2 = \frac{h_s}{k}\sqrt{\frac{\nu}{a}}.$$

The physical quantities of engineering interest, the friction factor, heat and mass transfer rate coefficients are given as:

$$C_f = 2\frac{\mu\frac{\partial u}{\partial y}}{\rho\,U_w^2}, \qquad Nu_x = \frac{(x+b)\frac{\partial T}{\partial y}}{T_w(x) - T_\infty}, \qquad Sh_x = \frac{(x+d)\frac{\partial C}{\partial y}}{C_w(x) - C_\infty}. \tag{17}$$

By using (5) and (6), Equation (17) becomes:

$$C_f(Re_x)^{0.5} = 2\left(\frac{m+1}{2}\right)^{0.5}\left((1+\beta^{-1})f''(0) + \Lambda\,f''^2(0)\right),$$

$$Nu_x = -\left(\frac{m+1}{2}\right)^{0.5}(Re_x)^{0.5}\theta'(0), \qquad Sh_x = -\left(\frac{m+1}{2}\right)^{0.5}(Re_x)^{0.5}\phi'(0), \tag{18}$$

where $Re_x = \frac{U_w X}{\nu}$ and $X = x + b$.

3. Procedure solution using Chebyshev spectral method

We solve the resulting system of non-linear ODEs of the form (11)-(13) with boundary conditions (14)-(15) by using the Chebyshev spectral method. For this purpose, since the Gauss-Lobatto nodes lie in the computational interval $[-1, 1]$, in the first step of this method, the transformation $\eta = \frac{\eta_\infty}{2}(x + 1)$ is used to change Equations (11) through (13) to the following form:

$$\left(1 + \frac{1}{\beta}\right)\left(\frac{2}{\eta_\infty}\right)^3 f''' + \left(\frac{2}{\eta_\infty}\right)^2\left(f''f - \left(\frac{2m}{m+1}\right)f'^2\right) + \Lambda\left(\frac{2}{\eta_\infty}\right)^5 f''f''' - M\left(\frac{2}{\eta_\infty}\right)f' = 0,$$
$$(19)$$

$$\left(\frac{2}{\eta_\infty}\right)^2 \theta'' - Pr\left(\frac{1-m}{m+1}\right)\left(\frac{2}{\eta_\infty}\right)f'\theta + Pr\left(\frac{2}{\eta_\infty}\right)f\theta' + Pr\, Du\left(\frac{2}{\eta_\infty}\right)^2 \phi'' = 0, \quad (20)$$

$$\left(\frac{2}{\eta_\infty}\right)^2 \phi'' - Sc\left(\frac{1-m}{m+1}\right)\left(\frac{2}{\eta_\infty}\right)f'\phi + Sc\left(\frac{2}{\eta_\infty}\right)f\phi' + Sc\, Sr\left(\frac{2}{\eta_\infty}\right)^2 \theta'' = 0, \quad (21)$$

with the following transformed boundary conditions:

$$\begin{aligned}
&f(-1) = 0, &&f'(-1) = 0, &&f'(1) = 0.5\,\eta_\infty, &&\theta'(-1) = 0.5\,\eta_\infty\,Bi1[1 - \theta(-1)], \\
&\theta(1) = 0, &&\phi'(-1) = 0.5\,\eta_\infty\,Bi2[1 - \phi(-1)], &&\phi(1) = 0,
\end{aligned} \quad (22)$$

where $f(x)$, $\theta(x)$, and $\phi(x)$ are the unknown functions from $C^m[-1, 1]$ and where the differentiation in the equations (19) through (21) will be for the new variable x. Our technique is accomplished by starting with a Chebyshev approximation for the highest order derivatives, $f^{(3)}$, $\theta^{(2)}$, and $\phi^{(2)}$ and generating approximations to the lower order derivatives $f^{(i)}$, $i = 0, 1, 2$ and $\theta^{(i)}$, $\phi^{(i)}$, $i = 0, 1$ as follows.

Setting $f^{(3)}(x) = \Omega(x)$, $\theta^{(2)}(x) = \Upsilon(x)$, and $\phi^{(2)}(x) = \xi(x)$, then by integration we obtain $f^{(2)}(x)$, $f^{(1)}(x)$, $f(x)$, $\theta^{(1)}(x)$, $\theta(x)$, $\phi^{(1)}(x)$, and $\phi(x)$ as follows:

$$\begin{aligned}
f^{(2)}(x) &= \int_{-1}^{x} \Omega(x)dx + c_0, \\
f^{(1)}(x) &= \int_{-1}^{x}\int_{-1}^{x} \Omega(x)dxdx + (x+1)c_0 + c_1, \\
f(x) &= \int_{-1}^{x}\int_{-1}^{x}\int_{-1}^{x} \Omega(x)dxdxdx + \frac{(x+1)^2}{2!}c_0 + \frac{(x+1)}{1!}c_1 + c_2,
\end{aligned} \quad (23)$$

Khader and Sharma: Evaluating the MHD Non-Newtonian Fluid Motion

AAM: Intern. J., Vol. 17, Issue 2 (December 2022)   427

$$\theta^{(1)}(x) = \int_{-1}^{x} \Upsilon(x)dx + d_0,$$

$$\theta(x) = \int_{-1}^{x} \int_{-1}^{x} \Upsilon(x)dxdx + (x+1)d_0 + d_1, \tag{24}$$

$$\phi^{(1)}(x) = \int_{-1}^{x} \xi(x)dx + e_0,$$

$$\phi(x) = \int_{-1}^{x} \int_{-1}^{x} \xi(x)dxdx + (x+1)e_0 + e_1. \tag{25}$$

From the boundary conditions (22), we can obtain the constants of integration $c_k, \ d_k, \ e_k, \ k = 0, 1, 2$, where

$$c_0 = \frac{\eta_\infty}{4} - \frac{1}{2}\int_{-1}^{1}\int_{-1}^{x}\Omega(x)dxdx, \qquad c_1 = 0, \qquad c_2 = 0,$$

$$d_0 = -\frac{Bi1}{2Bi1 - 1} - \frac{Bi1}{2Bi1 - 1}\int_{-1}^{1}\int_{-1}^{x}\Upsilon(x)dxdx, \quad d_1 = \frac{2Bi1}{2Bi1 - 1} + \frac{1}{2Bi1 - 1}\int_{-1}^{1}\int_{-1}^{x}\Upsilon(x)dxdx,$$

$$e_0 = -\frac{Bi2}{2Bi2 - 1} - \frac{Bi2}{2Bi2 - 1}\int_{-1}^{1}\int_{-1}^{x}\xi(x)dxdx, \quad e_1 = \frac{2Bi2}{2Bi2 - 1} + \frac{1}{2Bi2 - 1}\int_{-1}^{1}\int_{-1}^{x}\xi(x)dxdx.$$

Therefore, we can give approximations to the equations (19) through (21) as follows:

$$f_i = \sum_{j=0}^{n} \ell_{ij}^{f}\Omega_j + c_i^{f}, \qquad f_i^{(1)} = \sum_{j=0}^{n} \ell_{ij}^{f1}\Omega_j + c_i^{f1}, \qquad f_i^{(2)} = \sum_{j=0}^{n} \ell_{ij}^{f2}\Omega_j + c_i^{f2},$$

$$\theta_i = \sum_{j=0}^{n} \ell_{ij}^{\theta}\Upsilon_j + d_i^{\theta}, \qquad \theta_i^{(1)} = \sum_{j=0}^{n} \ell_{ij}^{\theta 1}\Upsilon_j + d_i^{\theta 1}, \tag{26}$$

$$\phi_i = \sum_{j=0}^{n} \ell_{ij}^{\phi}\xi_j + e_i^{\phi}, \qquad \phi_i^{(1)} = \sum_{j=0}^{n} \ell_{ij}^{\phi 1}\xi_j + e_i^{\phi 1},$$

for all $i = 0, 1, 2, ..., n$, where

$$\ell_{ij}^f = b_{ij}^3 - \frac{1}{4}(x_i + 1)^2 b_{nj}^2, \qquad \ell_{ij}^{f1} = b_{ij}^2 - \frac{1}{2}(x_i + 1)b_{nj}^2, \qquad \ell_{ij}^{f2} = b_{ij} - \frac{1}{2}b_{nj}^2,$$

$$\ell_{ij}^\theta = b_{ij}^2 - \frac{1}{2}(x_i + 1)b_{nj}^2, \qquad \ell_{ij}^{\theta1} = b_{ij} - \frac{1}{2}b_{nj}^2,$$

$$\ell_{ij}^\phi = b_{ij}^2 - \frac{1}{2}(x_i + 1)b_{nj}^2, \qquad \ell_{ij}^{\phi1} = b_{ij} - \frac{1}{2}b_{nj}^2,$$

$$c_i^f = \frac{\eta_\infty}{8}(x_i + 1)^2, \qquad c_i^{f1} = \frac{\eta_\infty}{4}(x_i + 1), \qquad c_i^{f2} = \frac{\eta_\infty}{4},$$

$$d_i^\theta = \frac{-Bi1}{2Bi1 - 1}(x_i + 1) + \frac{2Bi1}{2Bi1 - 1}, \qquad d_i^{\theta1} = \frac{-Bi1}{2Bi1 - 1},$$

$$e_i^\phi = \frac{-Bi2}{2Bi2 - 1}(x_i + 1) + \frac{2Bi2}{2Bi2 - 1}, \qquad e_i^{\phi1} = \frac{-Bi2}{2Bi2 - 1},$$

where $b_{ij}^2 = (x_i - x_j)b_{ij}$, $b_{ij}^3 = \frac{(x_i - x_j)^2}{2!}b_{ij}$, and b_{ij} are the elements of the matrix B as given in El-Gendi (1969). By using Equation (26), one can transform Equations (19) through (21) to the following system of non-linear equations in the highest derivative:

$$\left(1 + \frac{1}{\beta}\right)\Omega_i + \left(\frac{\eta_\infty}{2}\right)\left(f_i f_i^{(2)} - \left(\frac{2m}{m+1}\right)\left(f_i^{(1)}\right)^2\right) + \Lambda\left(\frac{2}{\eta_\infty}\right)^2 \Omega_i f_i^{(2)} - M\left(\frac{\eta_\infty}{2}\right)^2 f_i^{(1)} = 0,$$
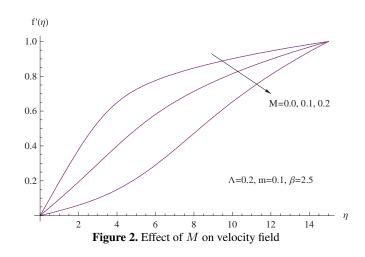(27)

$$\Upsilon_i - Pr\left(\frac{1-m}{m+1}\right)\left(\frac{\eta_\infty}{2}\right)f_i^{(1)}\theta_i + Pr\left(\frac{\eta_\infty}{2}\right)f_i\theta_i^{(1)} + Pr\,Du\,\xi_i = 0, \qquad (28)$$

$$\xi_i - Sc\left(\frac{1-m}{m+1}\right)\left(\frac{\eta_\infty}{2}\right)f_i^{(1)}\phi_i + Sc\left(\frac{\eta_\infty}{2}\right)f_i\phi_i^{(1)} + Sc\,Sr\,\Upsilon_i = 0. \qquad (29)$$

This scheme is a non-linear system of $3n + 3$ algebraic equations in $3n + 3$ unknowns Ω_i, Υ_i, and ξ_i, $(i = 0, 1, ..., n)$ which is then solved using the Newton iteration method. After solving this system and substituting Ω_i, Υ_i, and ξ_i in Equation (26), we can obtain the numerical solution of the system of equations (11) through (15).

Khader and Sharma: Evaluating the MHD Non-Newtonian Fluid Motion

AAM: Intern. J., Vol. 17, Issue 2 (December 2022)   429

4.   Results and discussion

The results obtained for Equations (11) through (13) along with the boundary conditions (14) through (15) for the non-Newtonian fluid flow are illustrated in Figures 2 through 16. Insofar as we are concerned with these governing equations, we note that this system cannot be solved analytically. So, we employ the Chebyshev spectral method to solve this system numerically. The variation of velocity with time for different values of the magnetic parameter M is studied in Figure 2.

Figure 2. Effect of M on velocity field

Here it is observed that as M increases impedance force is increasing, hence the velocity is decreased. Figures 3 and 4 underline the importance of the same magnetic parameter M and its effect on the dimensionless temperature and the dimensionless concentration, respectively. Here it is observed that both the temperature distribution and the concentration distribution are increasing as M is increasing. Hence, it can be concluded that both the sheet temperature $\theta(0)$ and the fluid concentration along the sheet $\phi(0)$ are maximum in case of maximum magnetic field strength and goes on decreasing as the magnetic field vanishing.
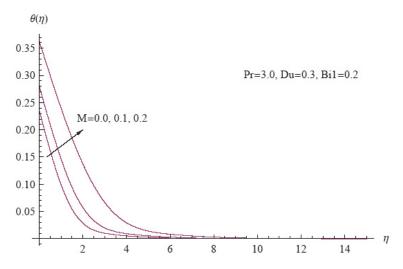
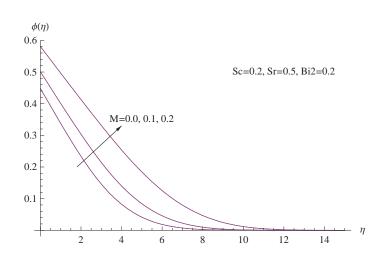**Figure 3.** Effect of M on temperature field

Figure 4. Effect of M on concentration field

In Figure 5, the dimensionless velocity profiles $f'(\eta)$ are drawn for various values of parameter m when $M = 0.1, \beta = 2.5$ and $\Lambda = 0.2$. As we see, the velocity decreases with increasing m which also produces larger values for the skin-friction as m enhances.
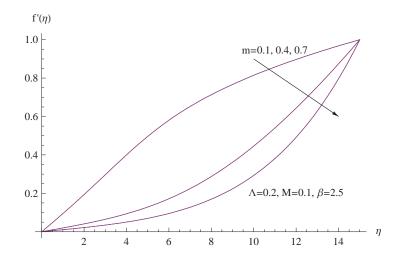

Figure 5. Effect of m on velocity field

On the other hand, for various values of m both the temperature profiles $\theta(\eta)$ and the concentration profiles $\phi(\eta)$ are shown in Figures 6 and 7, respectively. These figures show that the temperature at the surface $\theta(0)$ increases as m increases, which also agrees with the behavior of the concentration distribution presented in Figure 7. It should be mentioned that in the presence of small m, the thickness of both temperature layer and the concentration layer inside the boundary layer region become slight and tend to increase as m larger.
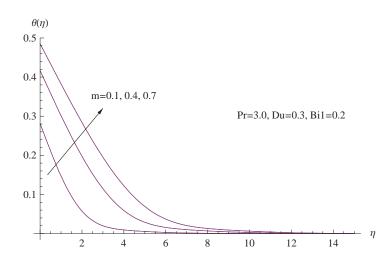
Khader and Sharma: Evaluating the MHD Non-Newtonian Fluid Motion

AAM: Intern. J., Vol. 17, Issue 2 (December 2022)   431

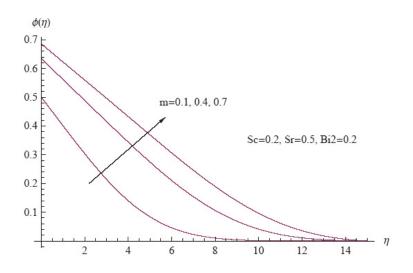**Figure 6.** Effect of m on temperature field

Figure 7. Effect of m on concentration field

The temperature profile $\theta(\eta)$ for various values of Sc is presented in Figure 8. This figure shows that the temperature at the surface is slightly large for large values of Sc which produces large heating for the sheet. The same behavior is noted inside the thermal region for increasing values of Sc.
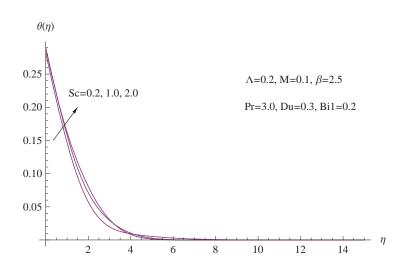
Figure 8. Effect of Sc on temperature field

One of the most important features of the model is that it allows to describing the concentration profile via the following Figure 9 along the stretching sheet for various values of Sc. This feature is not taken into account by the majority of the models in the literature. It is interesting to note that as Sc increases, the decrease of both the concentration layer thickness and the fluid concentration along the sheet $\phi(0)$ are greater.
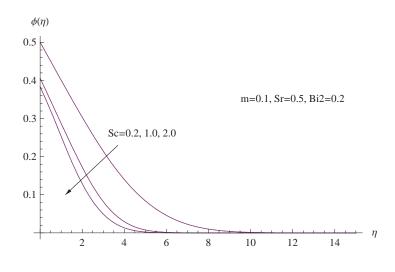

Figure 9. Effect of Sc on concentration field

The variation of temperature for different values of the Soret parameter Sr is introduced in Figure 10. From this figure, we observe that the effect of increase in Soret parameter, Sr under the application of the magnetic field is to decrease both the temperature distribution and the temperature at the surface $\theta(0)$.
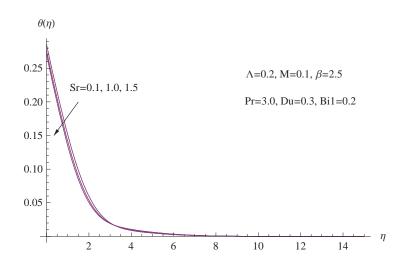
Khader and Sharma: Evaluating the MHD Non-Newtonian Fluid Motion

AAM: Intern. J., Vol. 17, Issue 2 (December 2022)   433

Figure 10. Effect of Sr on temperature field

Figure 11 depicts the effect of the Soret parameter Sr on the concentration profile $\phi(\eta)$ when other flow parameters are kept constant. It is observed that for a given position η, the concentration gets increased with an increase in Sr. In other words, increasing the Soret parameter Sr has the effect of increasing the fluid concentration along the sheet $\phi(0)$.
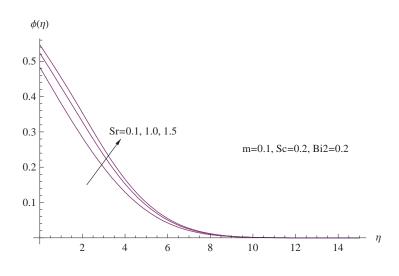

Figure 11. Effect of Sr on concentration field

Figure 12 indicates the variation of the temperature profile $\theta(\eta)$ with higher values of the Dufour parameter Du. It can be seen that even in presence of the magnetic field, as Du increases, the value of $\theta(\eta)$ increases for the same η. It is interesting to find that the temperature at the surface $\theta(0)$ increases with an increase in Du, as was expected. That is, the thermal boundary layer thickness turns out to be a monotonically increasing function of Du.
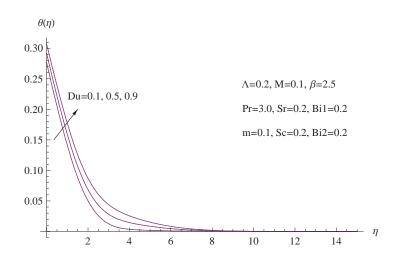
$\theta(\eta)$

Figure 12. Effect of Du on temperature field

To see the influence of the $Bi1$ on both the temperature and concentration fields, Figures 13 and 14 are plotted against η. The graphs show that with increasing $Bi1$, both the temperature and concentration distribution slightly increases.
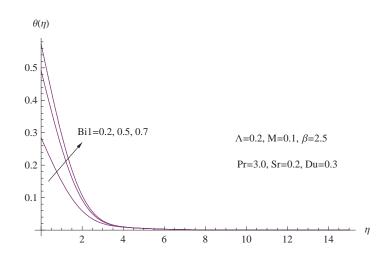
$\theta(\eta)$

Figure 13. Effect of $Bi1$ on temperature field

Khader and Sharma: Evaluating the MHD Non-Newtonian Fluid Motion

AAM: Intern. J., Vol. 17, Issue 2 (December 2022)   435
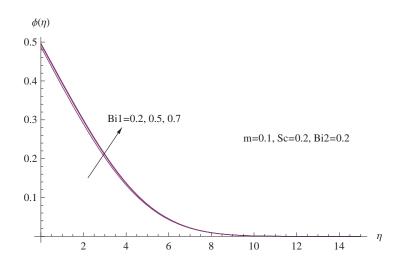

Figure 14. Effect of $Bi1$ on concentration field

Figures 15 and 16 show the same effect as said above but in the presence of $Bi2$ parameter. That is, an increase in $Bi2$ parameter leads in increase of both the temperature at the surface $\theta(0)$ and the fluid concentration along the sheet $\phi(0)$. Moreover, the concentration layer thickness becomes thicker for larger $Bi2$ parameter and a slight growth of temperature distribution in the boundary layer is given in Figure 15.
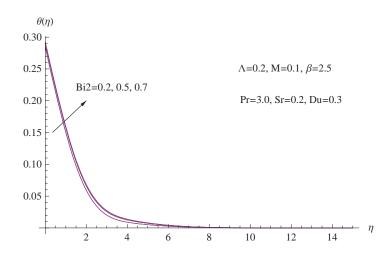

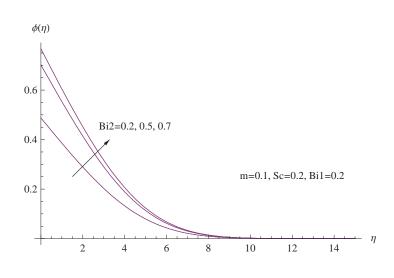**Figure 15.** Effect of $Bi2$ on temperature field

Figure 16. Effect of $Bi2$ on concentration field.

5. Concluding remarks

In the present work analysis, the MHD flow and the heat mass transfer within a boundary layer of non-Newtonian Casson/Williamson fluid above a stretching sheet is given. Numerical results by using the Chebyshev spectral collocation are presented to illustrate the details of the flow and heat transfer characteristics and their dependence on the various parameters. The results are presented graphically with various system parameters in detail.

The main findings of our study on the non-Newtonian fluid that moving over a stretching sheet are as follows:

(1) The dimensionless velocity at boundaries decreases with increasing the magnetic parameter and the stretching parameter.
(2) The effect of the magnetic field and the Dufour parameter on the fluid above the stretching sheet is to enhance the sheet temperature.
(3) The Soret parameter and the mass flux parameter have a prominent effect on the concentration field.
(4) When both the Casson parameter and the Williamson parameter are vanishes, results agree with those of Newtonian fluid.

Khader and Sharma: Evaluating the MHD Non-Newtonian Fluid Motion

AAM: Intern. J., Vol. 17, Issue 2 (December 2022)   437

REFERENCES

Anjali Devi, S.P. and Prakash, M. (2015). Temperature dependent viscosity and thermal conductivity effects on hydromagnetic flow over a slendering stretching sheet, J. Nigerian Math. Soc., Vol. 34, pp. 318–330.

Anjali Devi, S.P. and Prakash, M. (2016). Thermal radiation effects on hydromagnetic flow over a slendering stretching sheet, J. Braz. Soc. Mech. Sci. Eng., Vol. 38, pp. 423–431.

Bidemi, O.F. and Sami Ahamed, M.S. (2019). Soret and Dufour effects on unsteady Casson magneto-nanofluid flow over an inclined plate embedded in a porous medium, World Journal of Engineering, Vol. 16, pp. 260–274.

El-Gendi, S.E. (1969). Chebyshev solution of differential, integral and integro-differential equations, Computer J., Vol. 12, pp. 282–287.

Fang, T., Zhang, J. and Yao, S. (2009). Slip MHD viscous flow over a stretching sheet-an exact solution, Commun. Nonlinear Sci. Numer. Simul., Vol. 14, pp. 3731–3737.

Hayat, T., Saeed, Y., Asad, S. and Alsaedi, A. (2015). Soret and Dufour effects in the flow of Williamson fluid over an unsteady stretching surface with thermal radiation, J. Phys. Sci., Vol. 70, pp. 235–243.

Khader, M.M. (2011). On the numerical solutions for the fractional diffusion equation, Communications in Nonlinear Science and Numerical Simulation, Vol. 16, pp. 2535–2542.

Khader, M.M. (2013a). An efficient approximate method for solving linear fractional Klein- Gordon equation based on the generalized Laguerre polynomials, Inter. J. of Computer Mathematics, Vol. 90, pp. 1853–1864.

Khader, M.M. (2013b). The use of generalized Laguerre polynomials in spectral methods for fractional order delay differential equations, J. of Computational and Nonlinear Dynamics, Vol. 8, pp. 1–5.

Khader, M.M. and Abualnaja, K.M. (2019). Galerkin-FEM for obtaining the numerical solution of the linear fractional Klein-Gordon equation, J. of Applied Analysis and Computation, Vol. 9, pp. 261–270.

Khader, M.M. and Megahed, A.M. (2013). Numerical solution for boundary layer flow due to a nonlinearly stretching sheet with variable thickness and slip velocity, Eur. Phys. J. Plus, Vol. 128, pp. 100–108.

Khader, M.M. and Saad, K.M. (2018). A numerical approach for solving the problem of biological invasion (fractional Fisher equation) using Chebyshev spectral collocation method, Chaos, Solitons & Fractals, Vol. 110, pp. 169–177.

Khan, M.I., Waqas, M., Hayat, T. and Alsaedi, A. (2017). A comparative study of Casson fluid with homogeneous-heterogeneous reactions, J. of Colloid and Interface Science, Vol. 498, pp. 85–90.

Lawrence, L.L. (1967). Boundary layer over a thin needle, Phys. Fluids, Vol. 1, pp. 822–868.

Mahmoud, M.A.A. and Megahed, A.M. (2013). Thermal radiation effect on mixed convection heat and mass transfer of a non-Newtonian fluid over a vertical surface embedded in a porous medium in the presence of thermal diffusion and diffusion-thermo effects, J. of Applied Me-

chanics and Technical Physics, Vol. 54, pp. 90–99.

Mahmoud, M.A.A. and Megahed, A.M. (2017). MHD flow and heat transfer characteristics in a Casson liquid film towards an unsteady stretching sheet with temperature- dependent thermal conductivity, Brazilian Journal of Physics, Vol. 47, pp. 512–523.

Megahed, A.M. (2015a). Effect of slip velocity on Casson thin film flow and heat transfer due to an unsteady stretching sheet in the presence of variable heat flux and viscous dissipation, Applied Mathematics and Mechanics, Vol. 36, pp. 1273–1284.

Megahed, A.M. (2015b). MHD viscous Casson fluid flow and heat transfer with second- order slip velocity and thermal slip over a permeable stretching sheet in the presence of internal presence of internal heat generation/absorption and thermal radiation, Eur. Phys. J. Plus, Vol. 130, pp. 81–96.

Megahed, A.M. (2019). Williamson fluid flow due to a nonlinearly stretching sheet with viscous dissipation and thermal radiation, J. of the Egyptian Mathematical Society, Vol. 27, pp. 12–27.

Megahed, A.M. (2020). Steady flow of MHD Williamson fluid due to a continuously moving surface with viscous dissipation and slip velocity, Inter. J. of Modern Physics C, Vol. 31, pp. 1–12.

Nadeem, S. and Hussain, S.T. (2014). Flow and heat transfer analysis of Williamson nanofluid, Appl. Nanosci., Vol. 4, pp. 1005–1012.

Zehra, I. and Yousaf, M.M. and Nadeem, S. (2015). Numerical solutions of Williamson fluid with pressure dependent viscosity, Results Phys., Vol. 5, pp. 20–25.